LETTER

doi:10.1038/nature11358

More extreme swings of the South Pacific convergence zone due to greenhouse warming

Wenju Cai[1], Matthieu Lengaigne[2], Simon Borlace[1], Matthew Collins[3,4], Tim Cowan[1], Michael J. McPhaden[5], Axel Timmermann[6], Scott Power[7], Josephine Brown[7], Christophe Menkes[8], Arona Ngari[9], Emmanuel M. Vincent[2] & Matthew J. Widlansky[10]

The South Pacific convergence zone (SPCZ) is the Southern Hemisphere's most expansive and persistent rain band, extending from the equatorial western Pacific Ocean southeastward towards French Polynesia[1,2]. Owing to its strong rainfall gradient, a small displacement in the position of the SPCZ causes drastic changes to hydroclimatic conditions and the frequency of extreme weather events—such as droughts, floods and tropical cyclones—experienced by vulnerable island countries in the region[1–7]. The SPCZ position varies from its climatological mean location with the El Niño/Southern Oscillation (ENSO), moving a few degrees northward during moderate El Niño events and southward during La Niña events[2,5,6]. During strong El Niño events, however, the SPCZ undergoes an extreme swing—by up to ten degrees of latitude toward the Equator—and collapses to a more zonally oriented structure[5] with commensurately severe weather impacts[5,8–11]. Understanding changes in the characteristics of the SPCZ in a changing climate is therefore of broad scientific and socioeconomic interest. Here we present climate modelling evidence for a near doubling in the occurrences of zonal SPCZ events between the periods 1891–1990 and 1991–2090 in response to greenhouse warming, even in the absence of a consensus on how ENSO will change[12–14]. We estimate the increase in zonal SPCZ events from an aggregation of the climate models in the Coupled Model Intercomparison Project phases 3 and 5 (CMIP3[15] and CMIP5) multi-model database that are able to simulate such events. The change is caused by a projected enhanced equatorial warming in the Pacific[16] and may lead to more frequent occurrences of extreme events across the Pacific island nations most affected by zonal SPCZ events.

The SPCZ plays an important part in global circulation and is a major feature of the Southern Hemisphere's climate[1,2]. Its location largely controls rainfall, ocean circulation and tropical cyclogenesis patterns in the South Pacific[5–7]. The western, more equatorial portion of the SPCZ rainfall band is largely controlled by sea surface temperature (SST), whereas its eastern portion is also influenced by extratropical circulation and the subtropical dry zone of the southeastern Pacific[1,17]. As the SPCZ moves northward during El Niño events, countries located within the climatological SPCZ position experience forest fires and droughts[3,4] as well as an increased probability of tropical cyclone hits[5]. In addition, the associated environmental changes affect fisheries[18] and cause coral reef mortality through thermally induced coral bleaching[8–11] across the South Pacific. Observed zonal SPCZ events, characterized by a collapse of the meridional tilt of the rain band, often associated with an equatorward shift of the intertropical convergence zone, have occurred in conjunction with the strongest recorded El Niño events (for example, 1982/83, 1997/98), in which large SST anomalies develop in the central and eastern equatorial Pacific. The effects of these zonal SPCZ events are much more severe than those from weaker El Niño events, and include massive drought and food shortage[7], unprecedented coral bleaching-induced mortality[9,10] and cyclogenesis in the vicinity of French Polynesia[5], a region not accustomed to such occurrences.

These dramatic effects raise the question as to whether greenhouse warming will change the frequency of zonal SPCZ events. Although many studies have addressed the effects of a projected warming on the Pacific mean state[13,14,19,20], ENSO and its multiplicity[12–14,21,22] and the mean position of the SPCZ[23], the issue of how zonal SPCZ events will change in a warming climate has received little attention. Here we show that greenhouse warming leads to a significant increase in the frequency of such events.

We apply a multivariate signal processing method referred to as empirical orthogonal function (EOF) analysis to deconvolve the spatiotemporal rainfall variability into orthogonal modes, each described by a principal spatial pattern and an associated principal component time series[24]. For observations, we use the satellite-era rainfall data set[25] focusing on austral summer (December to February) when the SPCZ is best developed. The leading pattern (Fig. 1a) features opposite rainfall anomalies between the equatorial and southwestern Pacific around the climatological rain band position. The second pattern (Fig. 1b) is characterized by opposite rainfall anomalies in the equatorial western and central Pacific.

A nonlinear relationship exists between the two associated principal components (time series). In one cluster of events, the principal components are negatively correlated (blue, green and black dots in Fig. 1c) and rainfall anomalies embedded in the two patterns tend to offset each other east of the Date Line, resulting in rainfall variability located in the western Pacific. This cluster encompasses years characterized by the well-known northward and southward shift of the SPCZ during La Niña and moderate El Niño events, respectively (blue and green lines in Fig. 1a). In the second cluster, the principal components are both positive (red dots in Fig. 1c) and display a positive correlation, resulting in large precipitation anomalies east of the Date Line. This cluster consists of the three reported zonal SPCZ events[5] over the 1979–2011 period (1982/83, 1991/1992 and 1997/98, or one in 11 years) where the eastern portion moves equatorward by more than 10° in latitude (red line; Fig. 1b). A nonlinear relationship of the second principal component with a historical ENSO index (for example, Niño3.4) is apparent (Supplementary Fig. 1), although we do not distinguish the canonical from the Modoki[22] ENSO. We define a zonal SPCZ event as one for which the first principal component is greater than one standard deviation and the second principal component is greater than zero.

We use this nonlinear behaviour to assess the performance of 17 coupled general circulation models (CGCM) from the CMIP3[15] database forced with historical anthropogenic and natural forcings

[1]CSIRO Marine and Atmospheric Research, Aspendale, Victoria 3195, Australia. [2]Laboratoire d'Océanographie et du Climat: Expérimentation et Approches Numériques (LOCEAN), Tour 45-55 – 4ème étage – Pièce 408, Case 100 – UPMC, 4 Place Jussieu, 75252 Paris Cedex 05, France. [3]College of Engineering Mathematics and Physical Sciences, Harrison Building, Streatham Campus, University of Exeter, Exeter EX4 4QF, UK. [4]Met Office Hadley Centre, FitzRoy Road, Exeter EX1 3PB, UK. [5]NOAA/Pacific Marine Environmental Laboratory, Seattle, Washington 98115, USA. [6]IPRC, Department of Oceanography, SOEST, University of Hawaii, Honolulu, Hawaii 96822, USA. [7]Centre for Australian Weather and Climate Research, Bureau of Meteorology, Melbourne, Victoria 3001, Australia. [8]Institut de Recherche pour le Développement, 101 Promenade Roger Laroque, BP A5 – 98848, Noumea, New Caledonia. [9]Meteorological Service, PO Box 127, Avarua, Rarotonga, Cook Islands. [10]International Pacific Research Center, University of Hawaii at Manoa, Honolulu, Hawaii 96822, USA.

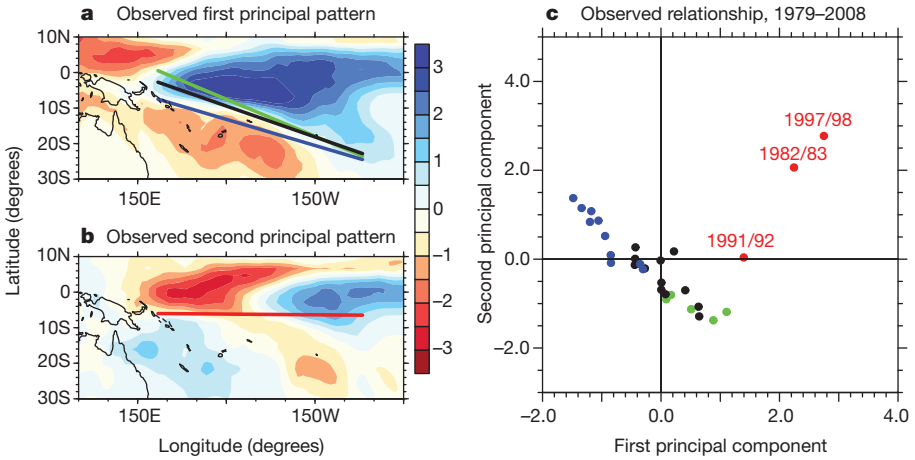

Figure 1 | Principal variability patterns of observed rainfall and their nonlinear relationship. **a**, **b**, Spatial patterns obtained by applying a statistical and signal processing method, EOF analysis[24], to a satellite-era rainfall anomaly data from the Global Precipitation Climatology Project version 2[25], focusing on the South Pacific domain (0°–30° S, 160° E–80° W) and the peak season for SPCZ, austral summer (December to February). The associated pattern beyond the domain is obtained by linearly regressing rainfall anomalies onto the time series. The first and second principal spatial patterns account for 47% and 16% of the total variance. The SPCZ position for El Niño (green line), La Niña (blue line) and neutral (black line) states is superimposed in **a**, and the position for zonal SPCZ events (red line) in **b**. The position of the SPCZ is defined as where the maximum rainfall is greater than 6 mm d^{-1} (ref. 5), and a linear fit is applied. Colour scale at right gives rainfall in mm d^{-1}; blue contours indicate increased rainfall, red contours indicate decreased rainfall per one standard deviation (s.d.) change. **c**, A nonlinear relationship between the associated principal component time series. La Niña, neutral and moderate El Niño years are indicated with blue, black and green dots, respectively. A zonal SPCZ event (red dots) is defined as when the first principal component is greater than one standard deviation, and when the second principal component is greater than zero. The different phases of ENSO events (El Niño and La Niña) are determined from a detrended Niño3.4 index when its amplitude is greater than 0.5 s.d.

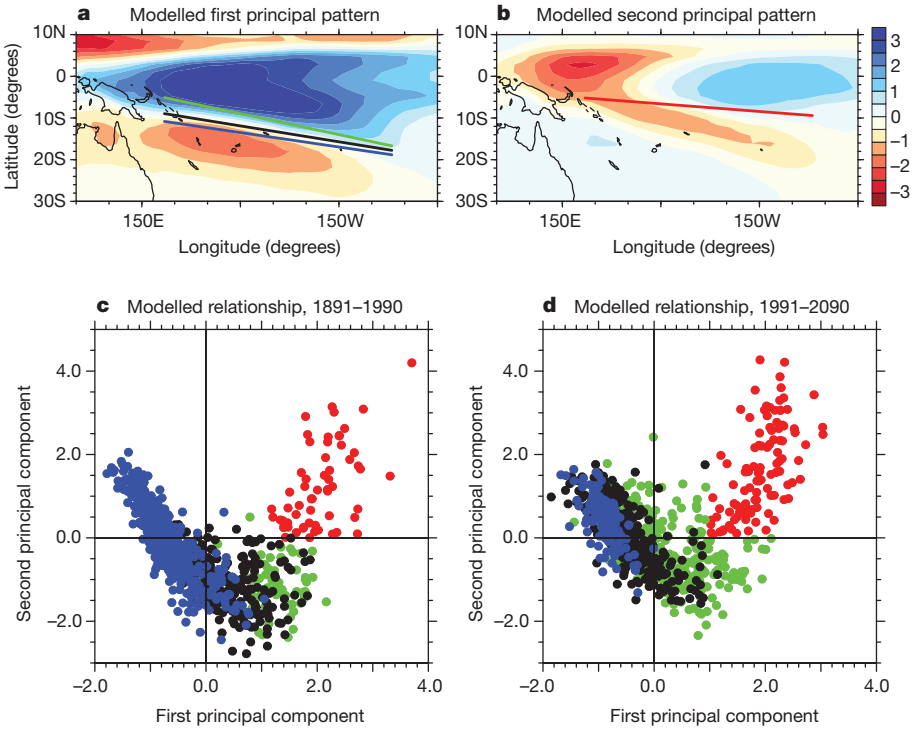

Figure 2 | Multi-model ensemble average of the principal variability patterns of rainfall and their nonlinear relationship from eight CMIP3 CGCMs that are able to produce the nonlinear relationship. **a**, **b**, The first (**a**) and second (**b**) principal variability patterns. The multi-model composite SPCZ position over the full 200 years of the control plus climate change periods (see below) for El Niño (green), La Niña (blue) and neutral (black) states is superimposed in **a**, and for zonal SPCZ events (red) in **b**. Colour scale at right gives rainfall in mm d^{-1}; blue contours indicate increased rainfall, and red contours indicate decreased rainfall per one s.d. change. **c**, **d**, The relationship between the associated two principal component time series for the control (1891–1990; **c**) and climate change (1991–2090; **d**) periods from the eight CMIP3 CGCMs. La Niña, neutral and moderate El Niño years are indicated with blue, black and green dots, respectively. Variance accounted for by the first and second principal pattern is model-dependent and ranges from 40–53% and 8–15% of the total variance, respectively. An increase in zonal SPCZ events (red dots) from the control to climate change period is evident from a comparison between **c** and **d**. An El Niño (or La Niña) is defined as when the detrended Niño3.4 index has an absolute value greater than 0.5 s.d.

before year 2000, and with a greenhouse gas emission scenario (SRESA2)[15] after year 2000 (see Methods). Nine models fail to generate the nonlinear behaviour (Supplementary Fig. 2). We focus on eight CGCMs that realistically simulate the two principal spatial patterns of rainfall anomalies (Fig. 2a and b), the nonlinear behaviour between the associated principal components (Fig. 2c and d), and the relationship with ENSO (Supplementary Figs 3 and 4). We compare the frequency of zonal SPCZ events in the first (1891–1990) and second (1991–2090) 100-year periods, which we refer to as the 'control' and the 'climate change' periods, respectively, to investigate the influence of greenhouse warming.

Aggregated over these eight CMIP3 CGCMs, the frequency of zonal SPCZ events increases by 81%, from about one event every 14 years in the control period to one every 7.5 years in the climate change period (Fig. 2c and d). This is statistically significant ($P < 0.001$) above the 99% confidence level based on a bootstrap test[26]. The statistical significance is underscored by a strong consensus among CGCMs, with six out of eight CGCMs simulating an increase in occurrences; a sensitivity test to varying definitions of zonal SPCZ events supports the robustness of our result (Supplementary Fig. 3 and Supplementary Table 1).

We conducted an identical analysis on rainfall outputs of 35 available experiments from 20 CMIP5 CGCMs under the historical emissions (before 2005) and a representative concentration pathway (RCP8.5, after 2005) scenario. Aggregated over 15 experiments from eight CMIP5 CGCMs that reproduce the nonlinear behaviour of the SPCZ, there is a similar increase in the occurrences of zonal SPCZ events, from one every 16 years in the control period to one every 7.5 years in the climate change period (Supplementary Table 2 and Supplementary Fig. 5).

We assess the potential impact of well-known biases in simulated climatological SSTs and SPCZ positions[23] using the HadCM3 CGCM (in which biases are corrected through a fixed flux adjustment[13]) in a set of 17 perturbed physics ensemble (PPE) climate change experiments forced with a 1% per year CO_2 increase. In these PPE experiments, perturbations are made to uncertain physical parameters within a single model structure. Aggregated over 12 experiments that produce the nonlinear behaviour of the SPCZ, there is a 214% increase in the frequency of zonal SPCZ events, from one event every 21 years in the control period to one event every 7 years in the climate change period (Supplementary Fig. 6 and Supplementary Table 3). Thus, the conclusions drawn from CMIP3 and CMIP5 CGCMs are not a consequence of the SST biases.

Understanding the relationship between the SPCZ and SST anomalies is crucial for unravelling the mechanism of the increase in zonal SPCZ events in a warming climate. To achieve this, modelled SST, wind and rainfall composite patterns are obtained for zonal SPCZ events (Fig. 3). In both periods, an eastward extension of the Pacific warm pool results in a substantial decrease of the meridional SST gradient south of the Equator, with a rainfall reduction over the western Pacific including northern Australia. In response, eastward-shifted westerly anomalies develop, with a maximum east of the Date Line and south of the Equator, accompanied by strong southeasterlies south of the warm SST anomalies (Fig. 3a and c), as in the observed SST and winds[5,27,28]. Such a wind response increases the moisture convergence east of the Date Line and south of the Equator, displacing the maximum moisture convergence and precipitation axis by up to 10° latitude to the north from its climatological position and contributing to the zonal orientation of the SPCZ (Fig. 3b and d). A zonal SPCZ event therefore occurs when the equatorial western Pacific moves from a state in which the off-equatorial region is warmer than the equatorial region to a condition in which the meridional SST gradient (the off-equatorial minus the equatorial) decreases considerably (Supplementary Figs 7 and 8). An increase in the frequency of zonal SPCZ events may hence arise from more frequent occurrences of a vanishing meridional SST gradient, which may be associated with a change in the occurrences of strong El Niño events. This mechanism also operates for the CMIP5 models for which data are available at the time of writing.

As shown in Supplementary Fig. 9, climate change (greenhouse warming) induces a larger warming rate along the Equator than in the off-equatorial central Pacific, a common feature of the response to global warming[16,29,30]. This pattern results in a slight decrease of the climatological meridional SST gradient in the central Pacific, which translates to an increase in the frequency of austral summers where the meridional SST gradient diminishes (for example, to a value <0.25 °C, Fig. 4a). Such a change occurs in all eight CMIP3 CGCMs (Fig. 4c), and in aggregation, the number of austral summers with a vanishing meridional SST gradient (that is, <0.25 °C) increases by 150%, from one every 15 summers during the control period to one every six summers during the climate change period. In association with this increase, for a given vanishing meridional SST gradient, the number of zonal SPCZ events increases (Fig. 4b).

In addition, there is a 32% increase in strong El Niño events (as measured by a Niño3.4 index greater than a 1.5-s.d. value; the Niño3.4

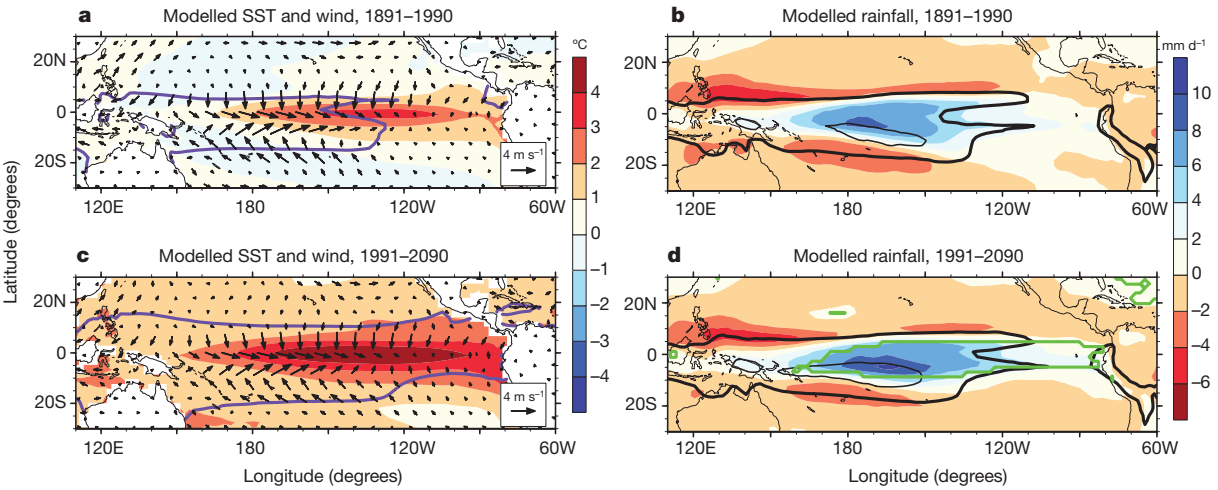

Figure 3 | Multi-model composites of the circulation fields associated with zonal SPCZ events. Shown are SST (°C), surface winds ($m\,s^{-1}$) and rainfall ($mm\,d^{-1}$) anomalies referenced to the mean climate of the control period. **a**, **b**, events over the control period; **c**, **d**, events over the climate change period. Contours of the composite 28 °C isotherm are superimposed on the SST anomalies (purple), and total rainfall of 6 $mm\,d^{-1}$ (thick black contour) and 12 $mm\,d^{-1}$ (thin black contour) are superimposed on the rainfall anomalies. The eight CMIP3 CGCM ensemble average shows an increase in rainfall intensity of ~10% averaged over the SPCZ area during such zonal SPCZ events, from the control period to the climate change period. In areas confined by the green curve, the increase is statistically significant ($P < 0.05$) above the 95% confidence level, based on a *t*-test comparing the two averages.

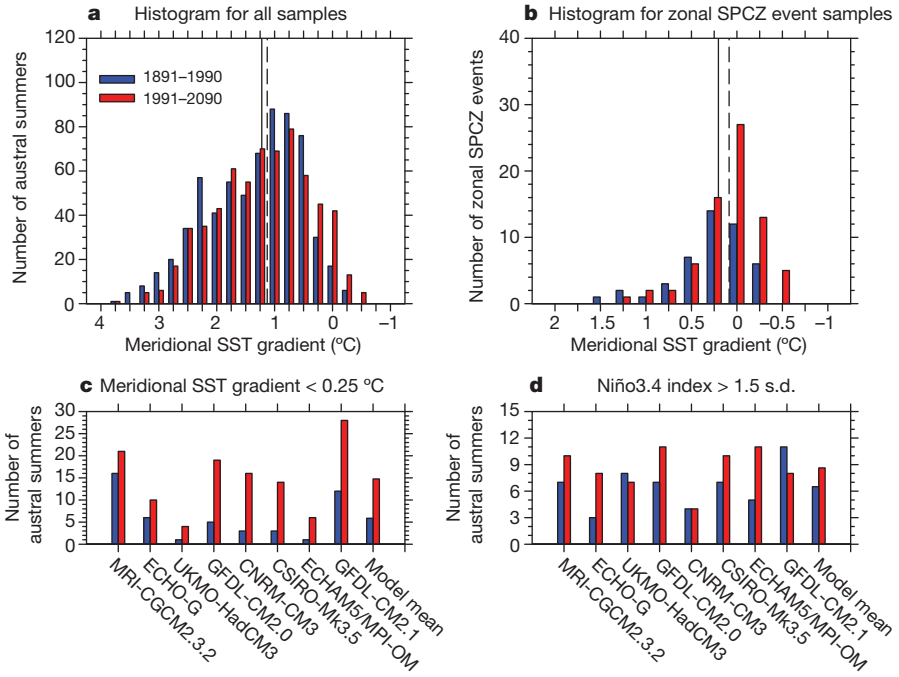

Figure 4 | Multi-model statistics associated with the increase in frequency of zonal SPCZ events. **a**, Multi-model histogram of the meridional SST gradient in the central equatorial Pacific for the eight CMIP3 CGCMs that are able to produce the nonlinear relationship for the control and climate change period. The meridional SST gradient is defined as the average SST over the off-equatorial region (10° S–5° S, 155° E–120° W) minus the average over the equatorial region (5° S-0°, 155° E–120° W). All 800 years in each period are separated in 0.25 °C bins centred at the tick point for the control (blue) and climate change (red) period. The multi-model median meridional SST gradient for the control (solid grey line) and the climate change (dashed grey line) periods are indicated. **b**, The same as **a** but for zonal SPCZ events only. Note that the horizontal axes in **a** and **b** are reversed; that is, decreasing go eastward. **c**, Changes in the number of austral summers in which the meridional SST difference virtually vanishes (that is, is <0.25 °C), with all eight CGCMs producing an increase. **d**, Changes in the number of strong El Niño events (the Niño3.4 index greater than a 1.5-s.d. value), with two CGCMs showing a decrease (UKMO-HadCM3 and GFDL-CM2.1).

index is defined as SST anomalies averaged over the region of 170° W–120° W, 5° S–5° N; Supplementary Table 4). This increase, seen in five out of eight CMIP3 CGCMs (Fig. 4d), occurs despite a tendency for a decrease in the total number of El Niño events (defined as when Niño3.4 is greater than a 0.5-s.d. or 0.75-s.d. value), and despite a general lack of consensus on how the El Niño amplitude may change[12,13]. However, only about 50% of the total increase in zonal SPCZ events coincides with a strong El Niño event, suggesting that such a change in El Niño is not necessary for an increase in zonal SPCZ events. Indeed, results from the 12 PPE experiments show a lack of consensus among the PPE experiments, despite a large increase in the frequency of zonal SPCZ events (Supplementary Fig. 10 and Supplementary Table 5), highlighting the fundamental importance of a decrease in the meridional SST gradient.

In summary, increased occurrences of zonal SPCZ events are consistent with the background state change in SST, and support our conclusion of an association with human-induced greenhouse warming, despite a lack of consensus on how ENSO will change. Although the simulated frequency in the control period is comparable to the observed frequency, the latter is based on observations over some three decades and may carry a large uncertainty. Thus, we cannot exclude the possibility that the observed frequency may be higher or lower if an extended observational record was available. With the projected large percentage increase, we expect more frequent occurrences of extreme events such as droughts, floods and tropical cyclones in the Pacific Island nations most affected by zonal SPCZ events.

METHODS SUMMARY

The zonal SPCZ events were diagnosed from observations and CGCMs. We propose an identification method based on the historical events, in which we apply EOF analysis[24] to the satellite-era austral summer rainfall anomalies for the 1979–2008 period over the South Pacific domain (160° E–80° W, 0°–30° S). The rainfall data[25], Global Precipitation Climatology Project monthly precipitation analysis, is obtained from http://www.esrl.noaa.gov/psd/data/gridded/data.gpcp.html. The rainfall anomalies are referenced to the climatological mean of the full period. This yields two leading patterns, one reflecting opposite rainfall anomalies between the equatorial and southwestern Pacific around the climatological rain band position, the other characterized by opposite rainfall anomalies in the equatorial western and central Pacific. The outputs of the analysis are arranged so that the principal component time series have a standard deviation of one, and the differences in variance are expressed in the pattern. Anomalies beyond the South Pacific domain are obtained by a linear regression. A zonal SPCZ event is defined as when the first leading time series is greater than one standard deviation, and when the second leading time series is greater than zero. This definition captures the three observed zonal SPCZ events in the second cluster. We also test the sensitivity of our results to varying definitions (Supplementary Table 1). The method is applied to rainfall anomalies of 17 CMIP3 CGCM simulations, each covering 110 years of a pre-twenty-first-century climate change simulation using historical anthropogenic and natural forcings (1891–2000) and another 90 years (2001–90; the longest common period for the CGCMs) from a future greenhouse warming simulation using the A2 greenhouse gas emission scenario (SRESA2)[15]. The same method is applied to 35 CMIP5 experiments under historical anthropogenic and natural forcings and the RCP8.5 forcing scenario, and 17 PPE experiments forced with historical and a 1% per year CO_2 increase, covering a 200-year period.

Full Methods and any associated references are available in the online version of the paper.

Received 11 April; accepted 27 June 2012.

1. Kiladis, G. N., Storch, H. V. & Loon, H. V. Origin of the South Pacific Convergence Zone. *J. Clim.* **2,** 1185–1195 (1989).
2. Vincent, D. G. The south Pacific convergence zone (SPCZ): a review. *Mon. Weath. Rev.* **122,** 1949–1970 (1994).
3. Salinger, M. J., Renwick, J. A. & Mullan, A. B. Interdecadal Pacific oscillation and South Pacific climate. *Int. J. Climatol.* **21,** 1705–1721 (2001).
4. Kumar, V. V., Deo, R. C. & Ramachandran, V. Total rain accumulation and rain-rate analysis for small tropical Pacific islands: a case study of Suva, Fiji. *Atmos. Sci. Lett.* **7,** 53–58 (2006).

5. Vincent, E. M. *et al.* Interannual variability of the South Pacific Convergence Zone and implications for tropical cyclone genesis. *Clim. Dyn.* **36,** 1881–1896 (2011).
6. Folland, C. K., Renwick, J. A., Salinger, M. J. & Mullan, A. B. Relative influence of the interdecadal Pacific oscillation and ENSO on the South Pacific Convergence Zone. *Geophys. Res. Lett.* **29,** 1643, http://dx.doi.org/10.1029/2001GL014201 (2002).
7. Hennessy, K. Power, S. & Cambers, G. (eds) *Climate Change in the Pacific: Scientific Assessment and New Research* Vol. 1, *Regional Overview*; Vol. 2, *Country Reports* (Australian Bureau of Meteorology and CSIRO, 2011).
8. Barnett, J. Dangerous climate change in Pacific Islands: food production and food security. *Reg. Environ. Change* **11,** 229–237 (2011).
9. Glynn, P. Widespread coral mortality and the 1982–83 El Niño warming event. *Environ. Conserv.* **11,** 133–146 (1984).
10. Hoegh-Guldberg, O. Climate change, coral beaching and the future of the world's coral reefs. *Mar. Freshwat. Res.* **50,** 839–866 (1999).
11. Mumby, P. J. *et al.* Unprecedented bleaching-induced mortality in *Porites* spp. at Rangiroa Atoll, French Polynesia. *Mar. Biol.* **139,** 183–189 (2001).
12. Guilyardi, E. *et al.* Understanding El Niño in ocean–atmosphere general circulation models: progress and challenges. *Bull. Am. Meteorol. Soc.* **90,** 325–340 (2009).
13. Collins, M. *et al.* The impact of global warming on the tropical Pacific Ocean and El Niño. *Nature Geosci.* **3,** 391–397 (2010).
14. Ashok, K., Sabin, T. P., Swapna, P. & Murtugudde, R. G. Is a global warming signature emerging in the tropical Pacific? *Geophys. Res. Lett.* **39,** L02701, http://dx.doi.org/10.1029/2011GL050232 (2012).
15. Meehl, G. *et al.* The WCRP CMIP3 multimodel dataset: a new era in climate change research. *Bull. Am. Meteorol. Soc.* **88,** 1383–1394 (2007).
16. Xie, S. P. *et al.* Global warming pattern formation: sea surface temperature and rainfall. *J. Clim.* **23,** 966–986 (2010).
17. Takahashi, K. & Battisti, D. S. Processes controlling the mean tropical Pacific precipitation pattern. Part II: the SPCZ and the southeast Pacific dry zone. *J. Clim.* **20,** 5696–5706 (2007).
18. Lehodey, P., Bertignac, M., Hampton, J., Lewis, A. & Picaut, J. El Niño Southern Oscillation and tuna in the western Pacific. *Nature* **389,** 715–718 (1997).
19. Cane, M. A. *et al.* Twentieth-century sea surface temperature trends. *Science* **275,** 957–960 (1997).
20. Vecchi, G. A. *et al.* Weakening of tropical Pacific atmospheric circulation due to anthropogenic forcing. *Nature* **441,** 73–76 (2006).
21. Yeh, S.-W. *et al.* El Niño in a changing climate. *Nature* **461,** 511–514 (2009).
22. Ashok, K., Behera, S. K., Rao, S. A., Weng, H. & Yamagata, T. El Niño Modoki and its possible teleconnection. *J. Geophys. Res.* **112,** C11007, http://dx.doi.org/10.1029/2006JC003798 (2007).
23. Brown, J. R., Moise, A. F. & Delage, F. P. Changes in the South Pacific Convergence Zone in IPCC AR4 future climate projections. *Clim. Dyn.* **39,** 1–19 (2012).
24. Lorenz, E. N. *Empirical Orthogonal Functions and Statistical Weather Prediction* (Statistical Forecast Project Rep. 1, Department of Meteorology, MIT, 1956).
25. Adler, R. F. *et al.* The version 2 Global Precipitation Climatology Project (GPCP) monthly precipitation analysis (1979-present). *J. Hydrometeorol.* **4,** 1147–1167 (2003).
26. Austin, P. C. Bootstrap methods for developing predictive models. *Am. Stat.* **58,** 131–137 (2004).
27. Spencer, H. Role of the atmosphere in seasonal phase locking of El Niño. *Geophys. Res. Lett.* **31,** L24104, http://dx.doi.org/10.1029/2004GL021619 (2004).
28. Lengaigne, M., Boulanger, J. P., Menkes, C. & Spencer, H. Influence of the seasonal cycle on the termination of El Niño events in a coupled general circulation model. *J. Clim.* **19,** 1850–1868 (2006).
29. Liu, Z., Vavrus, S., He, F., Wen, N. & Zhong, Y. Rethinking tropical ocean response to global warming: the enhanced equatorial warming. *J. Clim.* **18,** 4684–4700 (2005).
30. Timmermann, A., McGregor, S. & Jin, F.-F. Wind effects on past and future regional sea level trends in the southern Indo-Pacific. *J. Clim.* **23,** 4429–4437 (2010).

Supplementary Information is linked to the online version of the paper at www.nature.com/nature.

Acknowledgements This work was supported by the Australian Climate Change Science Program, CSIRO Office of Chief Executive Science Leader programme, and the Pacific-Australia Climate Change Science and Adaptation Planning Program. A.T. and M.J.W. were supported by the Office of Science (BER) US Department of Energy, grant DE-FG02-07ER64469, the US National Science Foundation under grant 1049219 and by the Japan Agency for Marine-Earth Science and Technology (JAMSTEC). M.J.M. was supported by NOAA and by CSIRO as a visiting scholar. M.L., C.M. and E.M.V. were supported by the Institut de Recherche pour le Développement (IRD). This is PMEL contribution number 3830.

Author Contributions W.C. and M.L. conceived the study, directed the analysis and wrote the initial draft of the paper. S.B. performed the analysis. M.C. conducted the perturbed physics ensemble climate change experiments with the HadCM3 model. All authors contributed to interpreting results, discussion of the associated statistical significance, and improvement of the paper.

Author Information Reprints and permissions information is available at www.nature.com/reprints. The authors declare no competing financial interests. Readers are welcome to comment on the online version of this article at www.nature.com/nature. Correspondence and requests for materials should be addressed to W.C. (wenju.cai@csiro.au).

METHODS

Selection of models. Whereas most of the comprehensive CGCMs are able to simulate the climatological mean SPCZ position and the relationship between the SPCZ and the ENSO[23], their ability to simulate the observed nonlinear relationship between the SPCZ and equatorial warming has not been assessed. An EOF analysis[24] is performed on the full 200 years of austral summer rainfall anomaly data from each of the 17 CMIP3 CGCMs[12]. The name of each CGCM is detailed in Supplementary Table 1. This analysis should yield two leading patterns, one reflecting opposite rainfall anomalies between the equatorial and southwestern Pacific around the climatological rain band position, the other characterized by opposite rainfall anomalies in the equatorial western and central Pacific. The relationship between the EOF1 and EOF2 time series should be nonlinear. A zonal SPCZ event is defined as when the first leading time series is greater than one standard deviation, and when the second leading time series is greater than zero. This definition captures the three observed zonal SPCZ events in the second cluster. Nine CGCMs fail to reproduce the observed feature in terms of a nonlinear relationship between EOF1 and EOF2 time series. These same nine models also poorly simulate the EOF2 pattern with contrasting anomalies over the equatorial western and central Pacific (Supplementary Fig. 2 and Supplementary Table 1). We therefore focus on the remaining eight models that do reproduce the observed nonlinear behaviour. Out of the 35 CMIP5 experiments from 20 CGCMs (available at the time of writing), only eight CGCMs with a total of 15 experiments produce the nonlinear behaviour of the SPCZ (Supplementary Table 2). Likewise, out of 17 PPE experiments, only 12 CGCMs simulate the observed nonlinearity of the SPCZ. Outputs from all experiments run from 1891 to 2090, under historical anthropogenic and natural forcings and then under projected climate scenarios. We derive changes in the occurrence of zonal SPCZ events by comparing the frequency of the first 100 years (control period) from that of the second 100 years (climate change period) in CGCMs that are able to produce zonal SPCZ events.

Statistical significance test. We use a bootstrap method[26] to examine whether the change in frequency of the zonal SPCZ events is statistically significant. The 800-year samples from the eight CMIP3 CGCMs in the control period are re-sampled randomly to construct another 5,000 realizations of 800-year records. During the random re-sampling process, overlapping is allowed, so that any one zonal SPCZ event can be selected again. The standard deviation of the zonal SPCZ frequency in the inter-realization is 7.4 events per 800 years, far smaller than the difference between the control and the climate change periods at 48 events per 800 years. The maximum frequency is 86, far smaller than that in the climate change period, further highlighting the strong statistical significance of the difference between the two periods. Increasing the realizations to 10,000 yields an essentially identical result. This process is repeated for the 15 CMIP5 experiments to create 10,000 realizations of 1,500 samples, and for the 12 PPE experiments to generate 10,000 realizations of 1,200 samples, from their respective control period. In both cases, the standard deviation of the zonal SPCZ frequency in the inter-realization is far smaller that the difference between the climate change and control period, while the maximum frequency of zonal SPCZ events is far smaller than that in the climate change period, indicating a strong statistical significance. The eight CMIP3 CGCM ensemble average shows a ~10% intensity rainfall increase over the SPCZ area, from the control period to the climate change period (Fig. 3d). We use a *t*-test to compare the two averages and to determine whether a statistically significance above the 95% confidence level is achieved.